# Augmenting Grid-based Contours to Improve Thin Plate DEM Generation

April 4, 2003

Michael B. Gousie
Department of Mathematics & Computer Science
Wheaton College
Norton, MA 02766

Wm. Randolph Franklin
Electrical, Computer, and Systems Engineering Department
Rensselaer Polytechnic Institute
Troy, NY 12180

**Abstract**

We present two new pre-processing techniques that improve thin plate Digital Elevation Model (DEM) approximations from grid-based contour data. One method computes gradients from an initial interpolated or approximated surface. The aspects are used to create gradient lines that are interpolated using Catmull-Rom splines. The computed elevations are added to the initial contour data set. Thin plate methods are applied to all of the data. The splines allow information to flow across contours, improving the final surface. The second method successively computes new, intermediate contours in between existing isolines, which provide additional data for subsequent thin plate processing. Both methods alleviate artifacts visible in previous thin plate methods. The surfaces are tested with published methods to show qualitative and quantitative improvements over previous methods.

# 1 Introduction

Geographical Information Systems (GIS) are becoming increasingly popular for visualizing spatial data. Most systems layer patterns or colors, which depict data such as soil type, roads, and the like, over a two-dimensional map. As technology continues to improve, users increasingly expect to view such data in three-dimensions, as is now done in ArcView and MapInfo. The user can then view the desired data in the context of the surrounding topology.

Digital Elevation Models (DEM) are often used to store three-dimensional elevation data via a regular grid. Because DEMs are not available for many areas and/or because they are storage intensive, they are often interpolated or approximated from sparse data. We have chosen isoline data from which to compute DEMs because contour maps are readily available for many geographic locations in the form of Digital Line Graphs (DLG), a standard of the United States Geological Survey (USGS). We use a grid-based approach because such methods often produce DEMs that preserve terrain morphology better than other methods, such as those using a Triangulated Irregular Network (TIN)(Jaakkola & Oksanen, 2000). Examples of systems that generate DEMs from contours are TOPOGRID (Hutchinson, 1988)(Hutchinson & Gallant, 1999), available in ArcInfo, TAPES-C (CRES, n.d.), and TOPOG (CSIRO, n.d.).

Although there are a myriad ways of interpolating or approximating a surface, we have concentrated our efforts on computing a smooth surface by minimizing its curvature. The partial differential equation (PDE) that models a thin plate being draped over the data points is one way to achieve such a surface. However, because thin plate surfaces minimize the curvature at known points, artifacts such as overshoot and terracing often result.

We wish to create surfaces that conform to the original contour data and that do not need any operator intervention, such as the addition of break lines or peaks. In this paper, we describe a new technique that computes "gradient lines" that follow the steepest slope. These lines are interpolated using Catmull-Rom splines to improve the subsequent thin plate approximation. A second technique computes "intermediate contours" which are used as additional data for a thin plate interpolation or approximation. The two methods are shown to produce surfaces that compare favorably, both qualitatively and quantitatively, to those created by previous thin plate procedures while adhering closely to the initial data.

# 2 Thin Plate Splines

Minimizing the curvature of the surface using a thin plate model is a common method for computing a DEM, and is available on commercial GIS products such as ArcView. In this section, we review the methods to which we compare our results. Additional thin plate methods are reviewed in the next two sections.

The notion of minimizing a thin plate to interpolate or approximate a surface is an old (i.e., (Briggs, 1974)) and trusted technique. Given $N$ data points, where $i \in \{1..N\}$, the

differential equation that models a thin plate is given by:

$$f_i = \int_R \int \left( f_{xx}^2 + 2f_{xy}^2 + f_{yy}^2 \right) dx\, dy \tag{1}$$

where $f_i$ is the force at position $i$. In practical terms, if the data is in the form of a mesh of points $(x_1, y_1)$ to $(x_n, y_n)$, and the boundaries are ignored, then using finite difference techniques, the solution to Equation 1 is the biharmonic equation (Briggs, 1974):

$$\begin{aligned} 0 \quad = \quad & z_{i-2,j} + z_{i,j-2} + z_{i+2,j} + z_{i,j+2} \\ & +2(z_{i-1,j-1} + z_{i-1,j+1} + z_{i+1,j+1} + z_{i+1,j-1}) \\ & -8(z_{i,j-1} + z_{i-1,j} + z_{i,j+1} + z_{i+1,j}) \\ & +20 z_{i,j} \end{aligned} \tag{2}$$

where each $z_{i,j}$ represents the elevation at $(x_i, y_j)$. The equation need only be solved if the value at a particular $z_{i,j}$ is unknown.

If an *approximation* is desired, then the computed surface must only pass near known values. In such a case, care must be taken so that the surface does not deviate too much from the known data values. Such an approximation can be modeled by adding (1) to a function which minimizes the total energy $E$ of a system (Jain, Kasturi & Schunck, 1995):

$$E^2 = \sum_{i=1}^{N} (z_i - f(x_i, y_i))^2 + \beta^2 \int_R \int \left( f_{xx}^2 + 2f_{xy}^2 + f_{yy}^2 \right) dx\, dy \tag{3}$$

where $\beta$ is a regularizing parameter used to achieve a smoother solution. Choosing a small $\beta$ results in a close approximation of the data, while choosing a large $\beta$ results in smoother solution.

A major source of difficulty in the production of smooth and accurate surfaces from sparse data using the thin plate approach is that the true terrain may itself exhibit discontinuities. For example, one such discontinuity may be described as a significant elevation drop between two flatter areas. This is often the case near cliffs or canyons. Because the thin plate method does not allow discontinuities, forcing the surface to be twice differentiable at control points ($C^2$ continuity), an "overshoot" results in the surface, known as Gibbs' phenomena (Foley, van Dam, Feiner & Hughes, 1990). Figure 1 shows a profile of a thin plate surface fit to elevations (vertical lines) that exhibits the problem.

To combat the effects of Gibbs' phenomena, tension is added to the biharmonic equation (Smith & Wessel, 1990):

$$E = \int_R \int \left( T_{xx} \frac{\partial^2 f}{\partial x^2} + 2T_{xy} \frac{\partial^2 f}{\partial x \partial y} + T_{yy} \frac{\partial^2 f}{\partial y^2} \right) dx\, dy \tag{4}$$

where $T_{xx}$, $T_{xy}$, and $T_{yy}$ represent horizontal forces per unit vertical length. The result is that unwanted inflections between sharp elevation changes are minimized, at the expense of localization of the curvature around the data points.

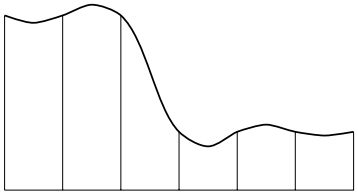

Figure 1: Profile (dark line) showing Gibbs' phenomena

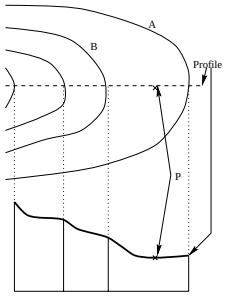


Figure 2: Profile (dark line) showing terracing problem in between contours

Although the thin plate equation has been used in the surface reconstruction problem, one problem manifests itself more often when using contour line data as opposed to scattered data. In simplest terms, a common solution to the thin plate equation at a particular node can be stated as the weighted average of the node's neighbors. Consider contour data depicting hilly or mountainous terrain. Furthermore, consider a contour line $A$ with a certain elevation, and a second contour line $B$ which is at the next higher elevation (see top of Figure 2). Typically, contour $A$ will have more data points than contour $B$, because the horizontal cross sections of mountains have less area as the elevation increases. This raises the problem that if one attempts to find the elevation of some point $p$, which lies between $A$ and $B$, then the number of elevation values whose magnitude is near the elevation of $A$ is greater than the number of elevation values whose magnitude is near the elevation of $B$. Using (2) to compute elevations between two such contours results in a "terracing" effect; that is, there are more lower elevation values than higher values, creating a surface whose average elevation is closer to $A$ than $B$ (bottom of Figure 2). The terracing looks more pronounced as the horizontal distance between successive contour lines increases (assuming the contours both curve in the same general direction). This behavior is intuitive, as a thin plate tends to planeness.

An important consideration in DEM production is how well the resulting surface is hydrologically accurate. Thin plate methods that generate terraces are poor for hydrological studies (Eklundh & Mårtensson, 1995). Hutchinson (Hutchinson, 1988) implemented a method that calculates a roughness penalty $J(f)$ composed of two partial differential equations:

$$J_1(f) = \int \left(f_x^2 + f_y^2\right) dx\, dy \tag{5}$$

$$J_2(f) = \int \left(f_{xx}^2 + 2f_{xy}^2 + f_{yy}^2\right) dx\, dy \tag{6}$$

$$J(f) = 0.5J_1(f) + J_2(f) \tag{7}$$

Furthermore, the algorithm enforces drainages by eliminating sinks and calculates ridges

and streams to facilitate the thin plate processing and to promote a hydrologically accurate model. This procedure is implemented in ArcInfo as TOPOGRID. Maunder (Maunder, 1999) increased the accuracy of computed flow lines and also determines pits and peaks in the contour data, but the method does not use thin plate splines to compute the DEM.

## 2.1 Additional Thin Plate Methods in Earth Sciences

A good overview of some of the first uses of minimum curvature can be found in (Schumaker, 1976). A discussion of the computational difficulties in interpolating many isolated points is found in (Powell, 1997), who also presents an iterative method for up to $10^5$ points.

In (Enriquez, Thomann & Goupillot, 1983), it is shown that minimizing a thin plate is an accurate method of interpolation. An improvement to Briggs' solution (Briggs, 1974) was presented in (Gonzalez-Casanova & Alvarez, 1985), which employed a more mathematically precise curvature minimization at the expense of run-time performance. A simpler algorithm was proposed in (Sandwell, 1987), using Green's functions instead of bicubic spline interpolation which makes the method more flexible because slope measurements can be used instead of elevation data. An example program using such interpolation is *Spherekit* (National Center for Cartographic Information and Analysis, 1996), which can handle up to 500 points per section.

Finally, ArcInfo's splining (thin plate) method produces good results in DEM gap fill applications (Doucette & Beard, 2000); it is not clear if these results reflect the output from ArcInfo's TOPOGRID procedure.

## 2.2 Use of Thin Plate Equations in Machine Vision

At the same time that research was on-going in the earth-sciences community, similar, relevant work was being done in the area of machine vision and surface reconstruction; see (Bolle & Vemuri, 1991) for a discussion of some of the various methods. Although many results seem to overlap those described above, there appears to be no direct link between the two groups. Much work in the vision area was done by Grimson (Grimson, 1983), who presented a theory of visual surface interpolation given stereo range data. He minimized the "quadratic variation" of the surface; this quadratic variation is exactly the thin plate equation, which he solved in a similar manner to Briggs.

Terzopoulos addressed the efficiency problems of Grimson's work by using the multigrid approach to solve essentially the same biharmonic equation (Terzopoulos, 1983*a*). However, a smoothness term is added to the quadratic functional, as shown as the $\beta$ term in Equation 3. This term models "springs" at the top of observed elevation values, allowing the thin plate to bend in a more natural way, reducing Gibbs' effects in the approximation.

In (Terzopoulos, 1983*b*, Terzopoulos, 1988), Terzopoulos gives a three-fold solution to the problems of depth and orientation discontinuities: In areas where there are no discontinuities, the problem reverts to the normal thin plate solution. Where there are depth

discontinuities in the surface, defined as occluding contours, the idea is to "break" the plate at the discontinuity, resulting in a piecewise continuous solution. Finally, orientation discontinuities, defined as surface creases, are handled by substituting a flexible membrane for the thin plate. The controlled-continuity stabilizer given in (Terzopoulos, 1988) is

$$\begin{aligned}\epsilon(v) &= \int_R \int \rho(x,y) \Big\{ \tau(x,y)(v_{xx}^2 + 2v_{xy}^2 + v_{yy}^2) \\ &\quad + [1 - \tau(x,y)](v_x^2 + v_y^2) \Big\}\, dx\, dy \end{aligned} \tag{8}$$

where $\rho(x,y)$ and $\tau(x,y)$ are continuity control functions, the former for depth discontinuities and the latter for orientation discontinuities. By varying the values of $\rho$ and $\tau$, the surface can behave as a membrane at one extreme or as a thin plate in complete tension at the other extreme (the tension parameter is very similar to that reported in (Smith & Wessel, 1990) later). A major problem of this approach is that the discontinuities must be known *a priori*. Terzopoulos handles this by comparing data from multiple sensors (Bolle & Vemuri, 1991). Such data is typically not available for the terrain modeler in GIS.

Another approach that deals with the discontinuity problem was given in (Jain et al. 1995, Sinha & Schunck, 1991, Sinha & Schunck, 1992). They use a two-stage process, where an initial surface based on the observed data is used to generate regular data using a moving least median squares regression (MLMS). The final surface is found by applying the energy functional:

$$E = \int_R \int \omega(x,y) \left( f_{xx}^2 + 2f_{xy}^2 + f_{yy}^2 \right) dx\, dy \tag{9}$$

where

$$\omega(x,y) = \frac{\beta^2}{1 + \|\rho(x,y)\|^2} \tag{10}$$

The smoothing term $\beta$ is the same as in Equation 3, while the value of $\rho(x,y)$ is the gradient, making the weight $\omega$ adaptive; it is large when the data is flat (small gradient), allowing the surface to be smoother. In steeper regions (large gradient), $\omega$ becomes large, which corresponds to a surface with many steep bends and pitches.

# 3 Improving Thin Plate Methods

Our approach to improving any of the thin plate methods is to add more, accurate elevation points into the initial contour data set, without the need for operator intervention (such as adding additional peak elevation data points). This results in a two-stage method where the contours are processed first, creating a richer data set. We create additional data through the use of "gradient lines" and "intermediate contours." The second stage applies any of the thin plate methods to yield the final surface.

Figure 3: A synthetic contour map

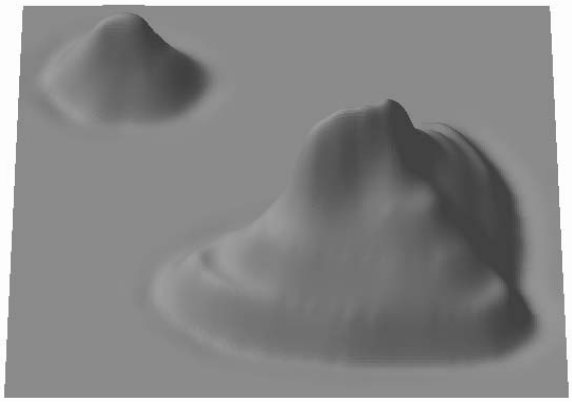

Figure 4: Thin plate surface approximation with $\beta = 0.5$

To compare our results to previous methods, we have implemented our own thin plate procedures. The "normal" thin plate method follows Briggs' equation (Equation 1), does not add tension or smooth the result, and produces a strict interpolation surface. Output generally resembles that of ArcView's splining function, although our method is more stable in that it does not produce large "spikes" in the computed surface that we have observed in some ArcView output. We have also implemented a thin plate approximation which models "springs" at the data points (Equation 3). A third version includes a tension parameter, following the equations in (Smith & Wessel, 1990) (Equation 4). Finally, we use ArcInfo's TOPOGRID (Hutchinson, 1988) for comparison purposes as well.

Consider a $257 \times 257$ raster file containing synthetic contours, shown in Figure 3. The thin plate approximation with springs produces the surface shown in Figure 4. Although the surface is generally smooth, one can see easily the terraces between contours and some Gibbs' phenomena at the lowest two contours on the left side of the larger hill. The use of tension, while helping to resolve the terracing problem, may produce radical changes in slope at contour lines and may flatten large areas, creating a scalloping effect between some contours and completely obliterating the rounded tops of hills. Some of these effects can be seen in Figure 5.

## 3.1 Gradient Lines

Intuitively, a better surface should be produced when given more data. One method, inspired by the concept of lofting in computer aided design (Faux & Pratt, 1981), computes "gradient lines" from local minima to maxima which intersect known contours perpendicularly. A similar idea is described in (Douglas, 1983), although the computation method is different. The gradient lines represent fall lines down the side of a hill. A fall line is the

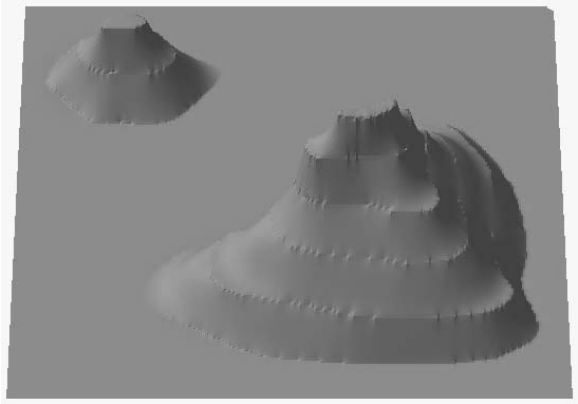

Figure 5: Thin plate under tension surface interpolation

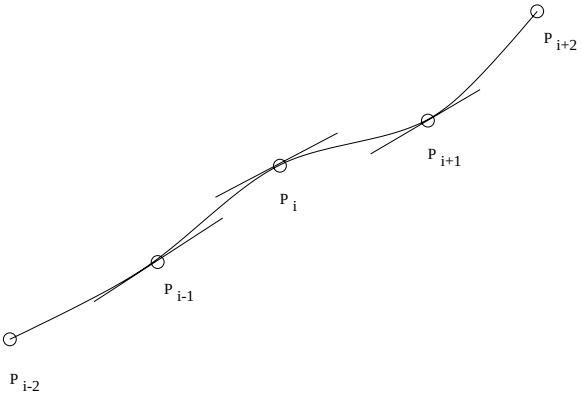


Figure 6: Catmull-Rom spline through contour elevations $P$. The straight line segments indicate the direction of the chord that connects adjacent points.

steepest route down a slope, or the path that a ball or water would take when descending from a particular point.

The gradient lines are formed by first computing an initial surface from which to calculate gradients; in our case, we used the normal thin plate interpolation. Approximate gradients are computed for each point on the grid from which the aspect is found easily (Skidmore, 1989). Using finite differences, the $x$ component of the gradient is:

$$\frac{1}{2}(z_{i+2,j} - z_{i-2,j} + z_{i+1,j-1} - z_{i-1,j-1} + z_{i+1,j+1} - z_{i-1,j+1} - 4z_{i+1,j} + 4z_{i-1,j}) \quad (11)$$

where each $z_{i,j}$ represents an elevation at grid location $(i, j)$ (Gousie & Franklin, 1998); the $y$ component is similar. A 2D path is formed from one grid location to another by following the direction of the gradient. Since the computations occur on a grid, the direction is rounded (within some threshold) to one of the eight cardinal directions, or one of the eight neighbors of an elevation point. If the direction is not rounded or the initial surface is horizontal at that location, then the grid point is not eligible to become part of a gradient line.

True elevations along a path are known only where it crosses contours. The unknown elevations are found by piecewise linear interpolation. An interpolating piecewise Catmull-Rom (Catmull & Rom, 1974, Farin, 1990) cubic spline, which has $C^1$ continuity, is fitted to each path, using the true elevations at contour crossings as control points. As shown in Figure 6, this spline passes through each control point $p_i$ in the direction parallel to the chord that runs through adjacent points $p_{i-1}$ and $p_{i+1}$. Since the control points are always situated on contours, the spline follows the slope trend of the previous and succeeding contours. Taking $P(u)$ as the representation for the parametric cubic point function for the curve section between the knots $p_i$ and $p_{i+1}$, the polynomial form of the spline is defined

by

$$P(u) = p_{i-1}(-\frac{1}{2}u^3 + u^2 - \frac{1}{2}u) + p_i(\frac{3}{2}u^3 - \frac{5}{2}u^2 + 1) + p_{i+1}(-\frac{3}{2}u^3 + 2u^2 + \frac{1}{2}u) + p_{i+2}(\frac{1}{2}u^3 - \frac{1}{2}u^2) \quad (12)$$

The algorithm for finding all of the gradient lines in a grid of contours is as follows:

Compute initial thin plate surface
Compute gradient at each grid point
For each point $P_{i,j}$ on the grid not visited
    create empty path
    repeat
        mark $P_{i,j}$ as visited
        add $P_{i,j}$ to path
        if $P_{i,j}$ contains a valid gradient direction
            move to neighboring point $P_{k,l}$ following gradient direction
    until there is no valid neighbor
    apply Catmull-Rom spline to path, using contour elevations as knots
    copy new computed elevations from path back to grid

Most of the surface will be covered by these paths, leaving some small gaps where the gradients were not found or did not follow one of the eight cardinal directions. A portion of the gradient lines computed from the synthetic data can be seen in Figure 7. The procedure would continue calculating more gradient lines at each point in the grid not previously processed. The result is a set of paths from local minima to maxima forming a rough surface through the contours. Because there is no provision for smoothing the surface between separate splines, or in areas not covered by splines (e.g. within closed contours), the second stage is to smooth the surface using the thin plate approximation, as shown in Figure 8.

## 3.2 Intermediate Contours

A property of contour lines is that, in general, successive lines run approximately parallel to one another. By finding data points in successive contour lines that are closest to one another, we can find a midpoint between the two contours. Repeating this process for all points along one contour will create a new "intermediate contour," which is in between the two existing contour lines. Furthermore, the elevation of the intermediate contour is exactly midway between the elevations of the original contours on either side. This can be assumed because the slope usually does not differ much from one contour to the next. The intermediate contours give a good approximation of the data values between observed values. This is especially helpful in areas where contours are spaced far apart. By incorporating the

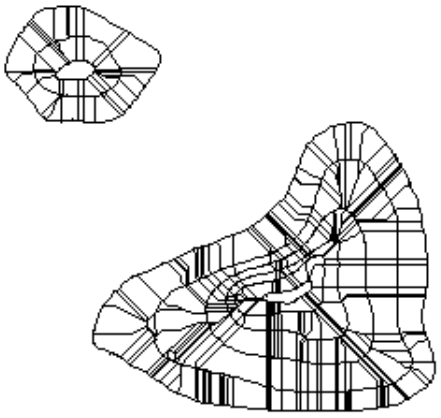

Figure 7: Synthetic data with gradient lines

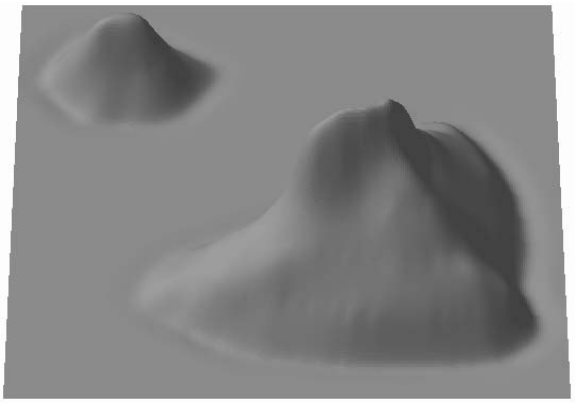

Figure 8: Thin plate surface approximation using gradient lines

intermediate contours in a thin plate approximation or interpolation, the terracing problem is much reduced. An additional benefit of creating such contours is that convergence of the thin plate algorithm may occur sooner, thus reducing total computation time. Finally, the additional contours are not considered to be original data, and thus are allowed to deviate from their computed elevations in later processing stages to yield a smooth surface.

Consider Figure 9. It depicts two contours which form a hill in the shape of a bean. This kind of shape is troublesome to minimum curvature methods because of the large areas devoid of contours at each end. Intermediate contours can help significantly because elevation values are found in the areas where there were no data points whatsoever, as shown in Figure 10.

Figure 9: A “bean” contour file

Figure 10: Bean with additional intermediate contour

Computing an intermediate contour is done through the following steps:
For all points P on contour lines

1. Choose a point $P_1$ from one contour line $A$

2. Find the closest point $P_2$ on contour line $B$ s.t. $B^{elevation} > A^{elevation}$

3. Determine the midpoint $P_{mid}$ between $P_1$ and $P_2$

4. Calculate elevation: $P_{mid}^{elevation} = \frac{1}{2}(P_1^{elevation} + P_2^{elevation})$

The condition shown in Step 2 that the elevations of neighboring contours differ assures that a new contour will have an elevation whose value is between the heights of its neighbors. Furthermore, this condition prevents the formation of a peak in a saddle area; such areas are computed in a later stage in the algorithm. Repeating the process whereby Step 2 finds the closest point such that $B^{elevation} < A^{elevation}$ results in fewer gaps in the intermediate contours. Bresenham's circle algorithm (Foley et al. 1990), which determines the points that best fit a circle with a given radius on a discrete grid, is employed to find the closest point $P_2$ from $P_1$. From $P_1$, circles with successively larger radii are generated until the circle contacts a point $P_2$ which has an elevation value higher or lower than $P_1$'s. The circular search is then terminated and the midpoint of the line that connects $P_1$ and $P_2$ is computed, rounded to the nearest grid position. The new elevation midway between the elevations of $P_1$ and $P_2$ is then stored at that location.

The algorithm can be repeated to compute as many intermediate contours as desired. Newly computed intermediate contour lines are included as data in successive iterations. Note that although this method is not optimal (see some gaps in the intermediate contours in Figure 10), two iterations of the algorithm are sufficient to reduce terracing effects in all of our tests. More iterations may be necessary if contours are very widely spaced. Another method to compute intermediate contours is to create the skeleton of the contours as shown in (Gold, 1999). Such a skeleton may create artificial peaks, such as in saddle areas, because no conditions on the elevations of contours are considered.

Using the synthetic data from Figure 3, two iterations of the intermediate contour method produces contours as shown in Figure 11. The thin plate approximation is applied to fill areas not yet computed and to promote a smooth surface. Figure 12 shows the surface computed from the contours shown in Figure 3. Because the computed intermediate contours introduce new elevation values into the initial data set, the resulting surface has fewer artifacts than a thin plate approximation alone.

# 4 Evaluation criteria

The two new algorithms were tested using data gathered from USGS sources. Our methods are compared to surfaces created with the thin plate with springs , the thin plate with tension, and the TOPOGRID procedure. Furthermore, since we wish to compare surfaces created with different methods using the same contour data, we assume the elevation data is reliable and concentrate on comparisons of the surfaces created from that data.

The criteria used to assess the quality of a computed DEM are as follows:

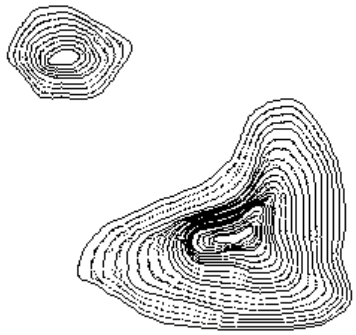

Figure 11: Synthetic data with two iterations of intermediate contours

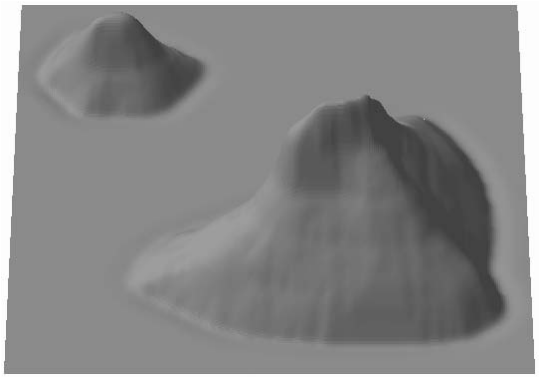

Figure 12: Surface approximation using intermediate contours

1. In general, the surface should look reasonably realistic with minimal artifacts. A shaded relief map is the conventional way to assess the surface visually (Wood & Fisher, 1993). Although this is a qualitative measure, it is very useful and may show artifacts that are not discovered easily through quantitative tests.

2. The total squared curvature must be as low as possible. Although natural surfaces exhibit some curvature, artifacts such as the aforementioned Gibbs' phenomena contribute greatly to the total curvature. For $N = n^2$ total points, this is found by comparing each computed elevation value to its four neighbors (Briggs, 1974):

$$C_{sq} = \sum_{i=2}^{n-1} \sum_{j=2}^{n-1} (u_{i+1,j} + u_{i-1,j} + u_{i,j+1} + u_{i,j-1} - 4u_{i,j})^2 \tag{13}$$

   where each $u$ represents the elevation at the grid location indexed by $i$ and $j$. The lower the squared curvature, the smoother the surface. This is useful for direct comparisons of results from different algorithms working on the same data.

3. The average absolute curvature must be as low as possible as well. Because small local imperfections may bias the total squared curvature, an average absolute curvature of the surface is computed:

$$C_{ave} = \frac{1}{(n-2)^2} \sum_{i=2}^{n-1} \sum_{j=2}^{n-1} |(u_{i+1,j} + u_{i-1,j} + u_{i,j+1} + u_{i,j-1} - 4u_{i,j})| \tag{14}$$

4. DEM elevations falling on the original contour lines must have values equal to (interpolation) or almost equal to (approximation) the contour labels (Carrara, Bitelli & Carla', 1997). This is measured by the root mean square error (*RMSE*) of the surface

(Rinehart & Coleman, 1988):

$$RMSE = \sqrt{\frac{1}{N}\sum_{i=1}^{N}(u_i - w_i)^2} \tag{15}$$

where $u_i$ = the interpolated DEM elevation of test point $i$
$w_i$ = the true elevation of test point $i$

Because most of the surfaces are the result of an approximation rather than a true interpolation, the *RMSE* refers to the error of the surface compared to the original contour map. Following (Carrara et al. 1997), an acceptable difference between a computed point and the contour elevation is five per cent of the contour interval. An *RMSE* of zero indicates a true interpolated surface.

The remaining tests are similar to those described in (Carrara et al. 1997). Additional methods for checking DEM accuracy, such as creating aspect maps for checking slope directions and using Laplacian filtering for edge detection, are found in (Wood & Fisher, 1993).

5. In an area bounded by a contour pair, the DEM elevations must fall within the elevations of the two contours. This can be done in a variety of ways, but one method to check for this criterion is to plot a profile of the surface in question. Although it shows only the elevations in one area, it is a reasonable test because thin plate methods find the minimum curvature surface globally, and thus one well-chosen profile will give a reasonable indication of the surface morphology between contours. It is also easy for the researcher to find patterns or artifacts in the surface quickly.

6. Within an area bounded by a contour pair, the DEM elevations should vary almost linearly. Although this is not true in all cases, in general a linear fit between contours indicates a constant slope and thus the absence of terracing artifacts.

   A method to determine this measure, used by (Carrara et al. 1997) and also (Reichenbach, Pike, Acevedo & Mark, 1993), is to group DEM elevations into integer intervals between two contours. These elevations are then reclassified into relative elevations. For example, if a contour pair were 100-120, then the relative elevations, or height classes, would be 0, 1, 2, ..., 19 corresponding to the actual elevations of 100, 101, 102, ..., 119. The height classes are computed for each elevation pair and then displayed as a histogram. A flat histogram indicates a smooth surface and a good linearity between the contours, while other patterns show various artifacts resulting from the particular interpolation or approximation method.

# 5 Results

The test case is shown in Figure 13, taken from a USGS DLG of Crater Lake, Oregon. The contours were rasterized into a $900 \times 900$ grid. Elevations are given in feet and the grid

spacing is in meters; the contour interval is 40 feet. As is evident in the contours, the Crater Lake data has both steep sections (rising from the lake in the lower left) and flatter sections, yielding a good test for reconstruction techniques.

Figure 13: $900 \times 900$ contours from a DLG of Crater Lake, OR

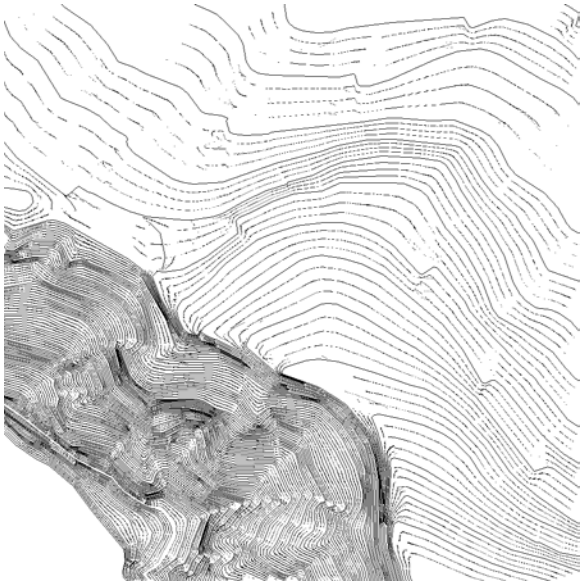

Figure 14: Two iterations of intermediate contours on Crater Lake data

Figure 15 shows the shaded relief map of our implementation of the thin plate with springs approximation. Without additional processing, this method yields terraces in the flatter sections because of the distance between contours, although the surface is visually acceptable in the steeper portions. Figure 16 shows the thin plate surface under tension. Between contours, the surface is quite smooth, but the addition of the tension parameter is not sufficient to eliminate the terracing problem. Furthermore, because this is a true interpolation, the original contour lines are clearly visible, even in the steeper sections. Figure 17 shows the surface produced by the TOPOGRID function, as implemented in ArcInfo. As with the previous method, the contour lines are clearly visible due to true interpolation, but the overall effect is much better. Note, however, several small dimples in the middle and south-east areas, as well as some ripples in the lower left corner, an area that represents the lake.

Figure 18 shows the gradient lines surface. The terracing is virtually eliminated, but there are small artifacts visible, yielding a slightly bumpy surface. These artifacts are the result of the failure of gradient lines to be produced in those areas because of the deficiencies of the initial thin plate surface used to generate gradients. The use of intermediate contours (Figures 14 and 19) also improves the flatter areas, although terracing remains a problem and there are additional small artifacts. The locations of these artifacts are similar to the gradient lines surface, implying that neither pre-processing method improved a

deficiency in the thin plate processing. Note that the TOPOGRID procedure successfully removed these spurious pits and peaks.

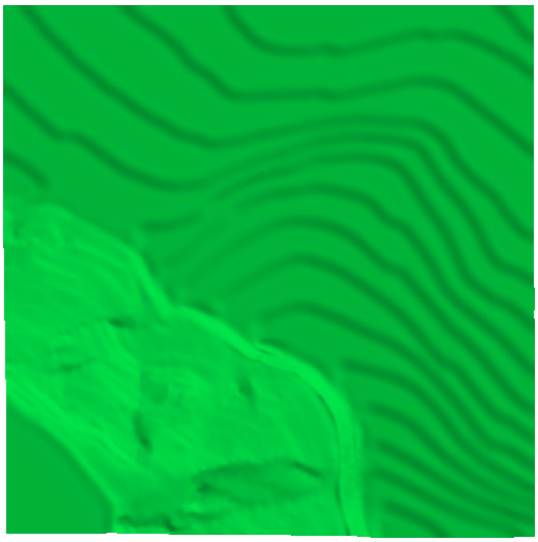

Figure 15: Shaded relief of Crater Lake DEM obtained from thin plate approximation

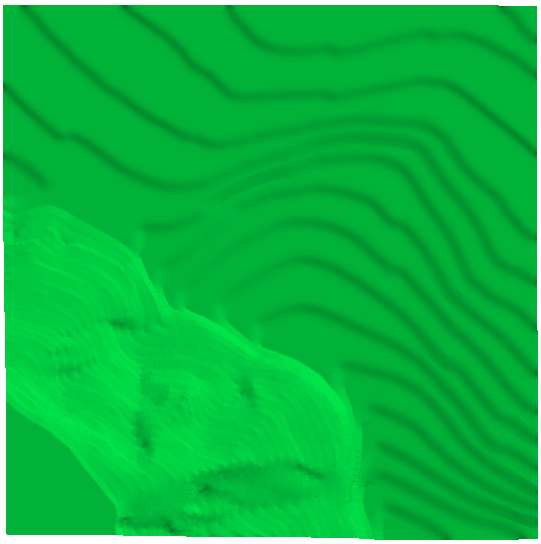

Figure 16: Crater Lake DEM obtained from thin plate under tension interpolation

The results of the quantitative tests two through four are shown in Table 1. The thin plate with springs approximation yields a total squared curvature of 72,678, which indicates a globally smooth surface in relation to the other surfaces. The average curvature is among the highest, however, suggesting that there must be large areas of high curvature which may be evidence of Gibbs' phenomena. The *RMSE* of 1.29 is 3.2% of the contour interval, which falls within the standard of five per cent used in (Carrara et al. 1997). Adding tension to the thin plate creates a true interpolation ( *RMSE* = 0), but at the cost of overall curvature. The TOPOGRID surface yields an *RMSE* of 3.62, which translates to 9.1% of the contour interval, significantly higher than the threshold of 5%. Although this is a interpolation method, the algorithm can change data points in order to enforce drainages and ridge lines, allowing for a non-zero *RMSE* . Visually, the gradient lines method produced a less-terraced surface, but with a few artifacts. This is borne out by the higher (than the thin plate approximation) total squared curvature, but the lower average curvature indicates that there are fewer large deviations. The statistics for the intermediate contours method are quite similar.

Criteria five indicates that elevations should always fall in between the heights of contour pairs. Plots of a diagonal (SW-NE) profile for all five methods on the Crater Lake data are shown in Figures 20 – 24. In all cases, the vertical lines indicate the heights of contours. Clearly, the thin plate approximation suffers not only from terracing, but also from Gibbs' phenomena, as the surface dips above and below the given contours. The thin

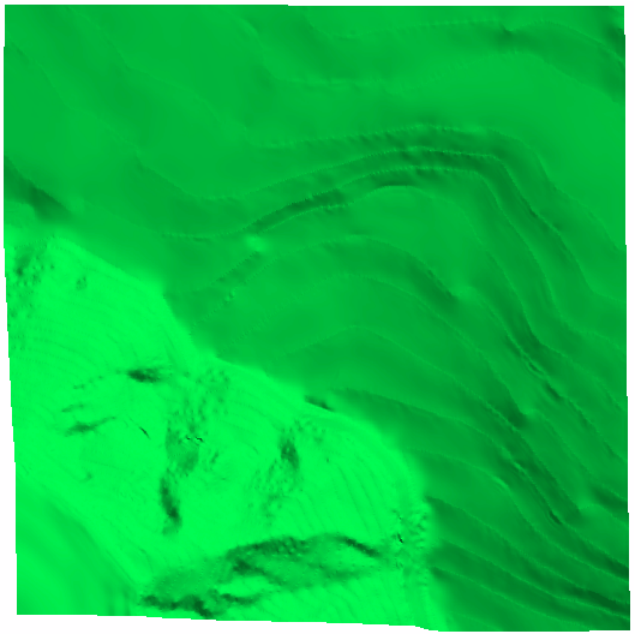

Figure 17: Crater Lake DEM obtained from ArcInfo's TOPOGRID procedure

plate under tension eliminates the Gibbs' phenomena, but the terracing is still in evidence. The TOPOGRID and the new methods follow the contours much better, but note that the lake is not quite flat.

Finally, to evaluate criteria six, plots were made of the relative heights of the DEMs of Crater Lake produced by each of the procedures. The plots can be seen in Figures 25 – 29. The frequency of the first height class for thin plate approximation is actually 235479; similarly, the frequency of the first height class for the thin plate under tension is 320682. Both of these indicate that the surfaces change rapidly right at the contour lines. The overall pattern of the graphs shows the terracing effect. In Figures 28 and 29, the frequency of the first height class is drastically reduced, but in both cases, there is still an artificially

Table 1: Results of applying methods to Crater Lake data.

| Method | $C_{sq}$ | $C_{ave}$ | *RMSE* | % of contour interval |
|---|---|---|---|---|
| Thin plate approximation | 72678 | 0.138 | 1.29 | 3.2 |
| Thin plate under tension interpolation | 741850 | 0.139 | 0.00 | 0.0 |
| TOPOGRID | 128100 | 0.144 | 3.62 | 9.1 |
| Gradient lines | 92800 | 0.117 | 1.29 | 3.2 |
| Intermediate contours | 92788 | 0.118 | 1.93 | 4.8 |

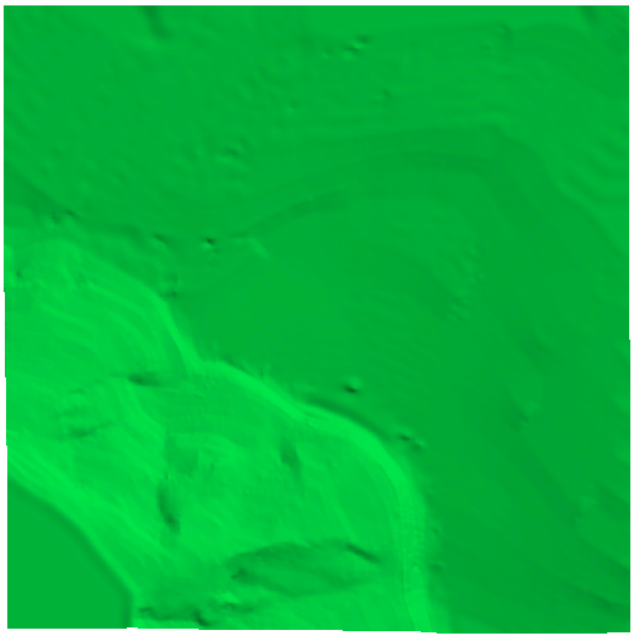

Figure 18: Crater Lake DEM obtained from gradient lines procedure

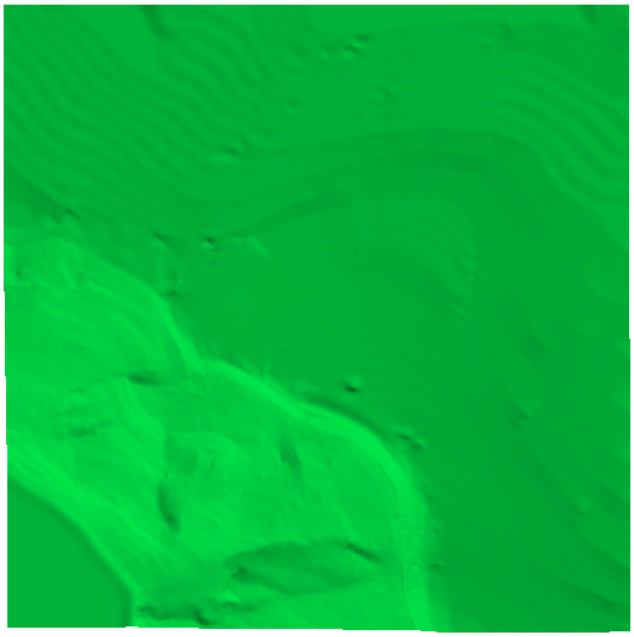

Figure 19: Crater Lake DEM obtained from intermediate contours and thin plate approximation

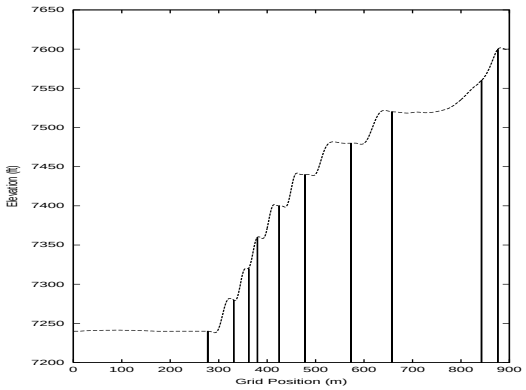


Figure 20: Thin plate approximation

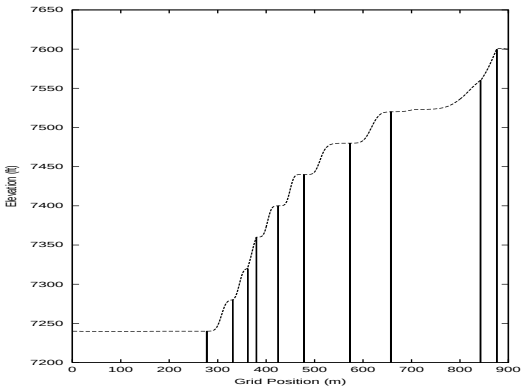


Figure 21: Thin plate under tension

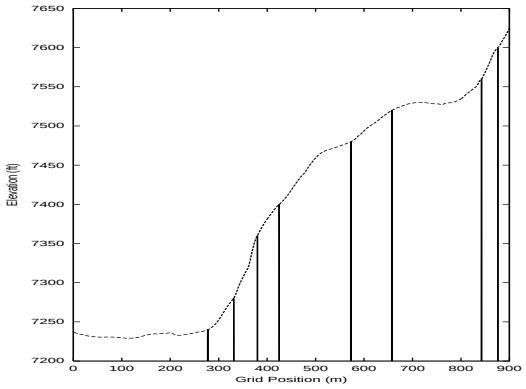


Figure 22: TOPOGRID

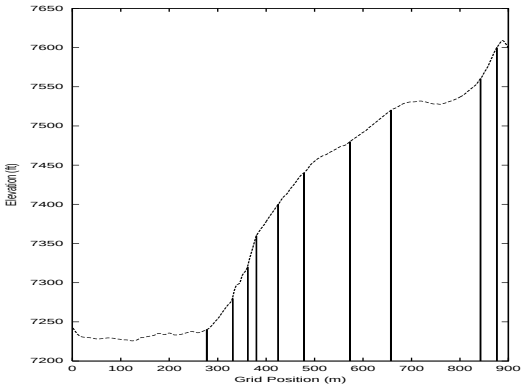


Figure 23: Thin plate with gradient lines

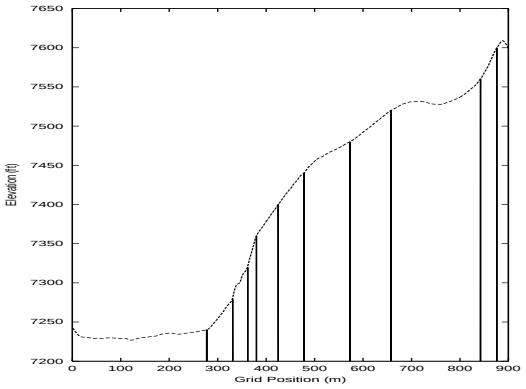


Figure 24: Thin plate with intermediate contours

introduced pattern, probably indicating the presence of terracing but at a smaller scale. The TOPOGRID procedure shows a very regular pattern. The three elevated bars in the intermediate contours method plot clearly show problems arising from the two iterations of the algorithm, which would produce three new contours: the first (at $x = 20$) in the middle of the original contours (at 0 and 39) and the next two from inserting a new contour in between 0 and 20 and again between 20 and 39. The artifacts near these latter contours are shown as the elevated bars at 10 and 30, respectively.

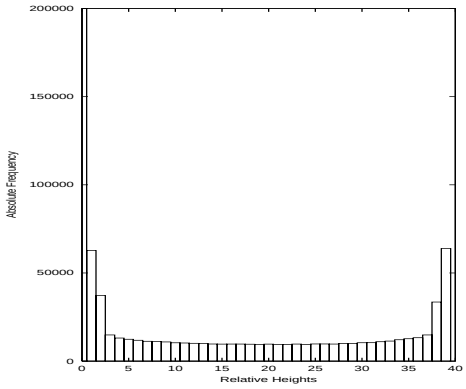


Figure 25: Thin plate approximation

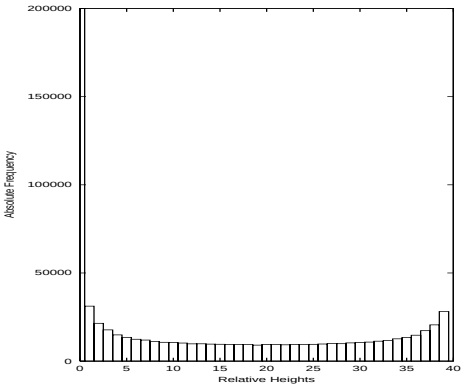


Figure 26: Thin plate under tension

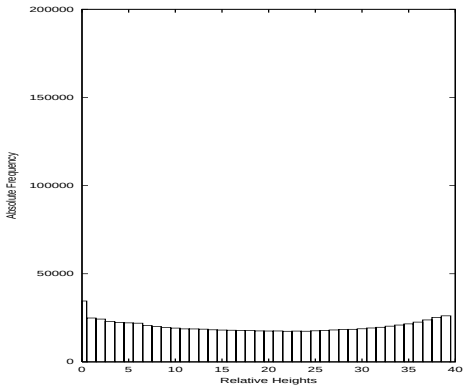


Figure 27: TOPOGRID

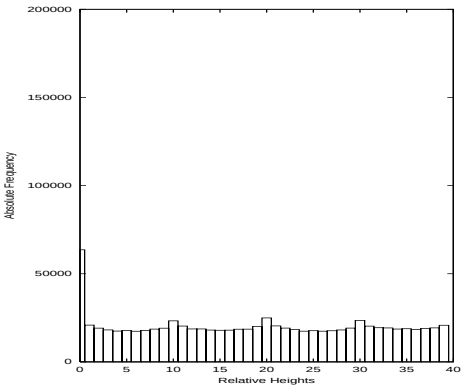


Figure 28: Thin plate with gradient lines

# 6 Conclusions

The thin plate interpolation, approximation, or the addition of tension may compute smooth DEMs from contour input, but often Gibbs' phenomena and especially terracing effects are

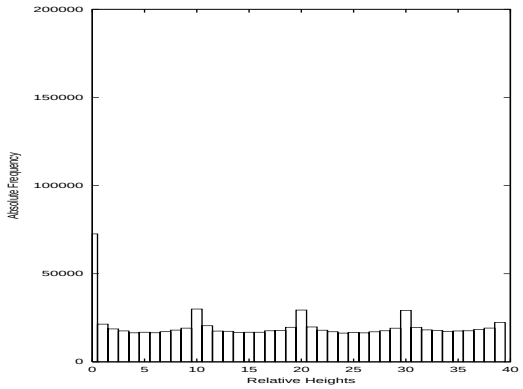


Figure 29: Thin plate with intermediate contours

visible. The problem worsen as contour spacing increases, and is readily apparent in shaded relief maps. Automatically adding additional data in a pre-processing step through either gradient lines or intermediate contours visually improve the surface created by subsequent thin plate processing, compared to thin plate methods alone. In all cases, the new methods produce smooth surfaces as shown by the total squared curvature and average curvature, while still being faithful to the original contour data, as measured by the *RMSE* . The profiles and height class plots show that the new methods create better surfaces in between contours than previous thin plate procedures alone. The surfaces compare favorably to ArcInfo's TOPOGRID procedure, the latter of which exhibited a much higher *RMSE* . Furthermore, no special operator input, such as break lines or peaks, is needed for the new methods.

Although the final DEMs created using the new methods are shown to be better generally than previous thin plate results, there is still room for improvement. Small artifacts may be seen in some of the computed surfaces, especially in flatter areas. This is especially true of the gradient lines method which relies on a preliminary thin plate surface. Both new methods should be improved to eliminate small gaps that are not well handled by subsequent thin plate procedures.

# References


Bolle, R. M. and Vemuri, B. C., 1991, On three-dimensional surface reconstruction methods, IEEE Transactions on Pattern Analysis and Machine Intelligence 13(1):1–13.

Briggs, I., 1974, Machine contouring using minimum curvature, Geophysics 39(1):39–48.

Carrara, A., Bitelli, G. and Carla', R., 1997, Comparison of techniques for generating digital terrain models from contour lines, International Journal of Geographical Information Science 11(5):451–473.

Catmull, E. and Rom, R., 1974, A class of local interpolating splines, Computer Aided Geometric Design (R. Barnhill and R. Riesenfeld, editors), Academic Press, pp. 317–326.

CRES, n.d., TAPES: Terrain programs for the environmental sciences, URL: http://cres.anu.edu.au/outputs/tapes.html.

CSIRO, n.d., TOPOG, URL: http://www.clw.csiro.au/topog/.

Doucette, P. and Beard, K., 2000, Exploring the capability of some GIS surface interpolators for DEM gap fill, Photogrammetric Engineering and Remote Sensing 66(7):881–888.

Douglas, D. H., 1983, The XYNIMAP family of programs for geographic information processing and thematic map production, Auto–Carto 6:Sixth International Symposium on Computer-Assisted Cartography (B. S. Wellar, editor), Vol. 2, pp. 2–14.

Eklundh, L. and Mårtensson, U., 1995, Rapid generation of digital elevation models from topographic maps, International Journal of Geographical Information Systems 9(3):329–340.

Enriquez, J. O. C., Thomann, J. and Goupillot, M., 1983, Applications of bidimensional spline functions to geophysics, Geophysics 48(9):1269–1273.

Farin, G., 1990, Curves and Surfaces for Computer Aided Geometric Design: A Practical Guide, 2 edn, Academic Press, Inc.

Faux, I. and Pratt, M., 1981, Computational Geometry for Design and Manufacture, Mathematics and its applications, Halsted Press.

Foley, J. D., van Dam, A., Feiner, S. K. and Hughes, J. F., 1990, Computer Graphics: Principles and Practice, 2 edn, Addison Wesley.

Gold, C. M., 1999, Crust and anti-crust: A one-step boundary and skeleton extraction algorithm, Symposium on Computational Geometry, pp. 189–196. citeseer.nj.nec.com/100454.html.

Gonzalez-Casanova, P. and Alvarez, R., 1985, Splines in geophysics, Geophysics 50(12):2831–2848.

Gousie, M. B. and Franklin, W. R., 1998, Converting elevation contours to a grid, Eighth International Symposium on Spatial Data Handling (T. Poiker and N. Chrisman, editors), pp. 647–656.

Grimson, W., 1983, An implementation of a computational theory of visual surface interpolation, Computer Vision, Graphics, and Image Processing 22:39–69.

Hutchinson, M. F., 1988, Calculation of hydrologically sound digital elevation models, Proceedings of the Third International Symposium on Spatial Data Handling, International Geographical Union, Columbus, Ohio, pp. 117–133.

Hutchinson, M. F. and Gallant, J. C., 1999, Representation of terrain, Geographical Information Systems: Principles and Technical Issues (Longley, Goodchild, Maguire and Rhind, editors), 2 edn, Vol. 1, Wiley, pp. 105–124.

Jaakkola, O. and Oksanen, J., 2000, Creating DEMs from contour lines: Interpolation techniques which save terrain morphology, GIM International 14(9):46–49.

Jain, R., Kasturi, R. and Schunck, B. G., 1995, Machine Vision, McGraw Hill, New York.

Maunder, C. J., 1999, An automated method for constructing contour-based digital elevation models, Water Resources Research 35(12):3931–3940.

National Center for Cartographic Information and Analysis, 1996, SphereKit, URL: http://ncgia.ucsb.edu/pubs/spherekit.

Powell, M., 1997, Thin plate spline interpolation in two dimensions, CTAC97, The eighth biennial Computational Techniques and Applications Conference, Computational Mathematics Group of Australian and New Zealand Industrial and Applied Mathematics Society (ANZIAM), a Division of the Australian Mathematical Society.

Reichenbach, P., Pike, R. J., Acevedo, W. and Mark, R. K., 1993, A new landform map of italy in computer-shaded relief, Bollettino Geodesia a Scienze Affini 52:22–44.

Rinehart, R. E. and Coleman, E. J., 1988, Digital elevation models produced from digital line graphs, Proceedings of the ACSM-ASPRS Annual Convention, Vol. 2, American Congress on Surveying and Mapping, American Society for Photogrammetry and Remote Sensing, pp. 291–299.

Sandwell, D. T., 1987, Biharmonic spline interpolation of Geos-3 and SEASAT altimeter data, Geophysical Research Letters 14(2):139–142.

Schumaker, L. L., 1976, Fitting surfaces to scattered data, Approximation Theory II (G. G. Lorentz, C. Chui and L. L. Schumaker, editors), Academic Press, pp. 203–268.

Sinha, S. S. and Schunck, B. G., 1991, Surface approximation using weighted splines, Proceedings IEEE Conference on Computer Vision and Pattern Recognition, IEEE, pp. 44–49.

Sinha, S. S. and Schunck, B. G., 1992, A two-stage algorithm for discontinuity-preserving surface reconstruction, IEEE Transactions on Pattern Analysis and Machine Intelligence 14(1):36–57.

Skidmore, A. K., 1989, A comparison of techniques for calculating gradient and aspect from a digital elevation model, International Journal of Geographical Information Systems 3(4):323–334.

Smith, W. H. F. and Wessel, P., 1990, Gridding with continuous curvature splines in tension, Geophysics 55(3):293–305.

Terzopoulos, D., 1983*a*, Multilevel computational processes for visual surface reconstruction, Computer Vision, Graphics, and Image Processing 24:52–96.

Terzopoulos, D., 1983*b*, The role of constraints and discontinuities in visible-surface reconstruction, Proceedings of the Eighth International Joint Conference on Artificial Intelligence, pp. 1073–1077.

Terzopoulos, D., 1988, The computation of visible-surface representations, IEEE Transactions on Pattern Analysis and Machine Intelligence 10(4):417–438.

Wood, J. D. and Fisher, P. F., 1993, Assessing interpolation accuracy in elevation models, IEEE Computer Graphics and Applications pp. 48–56.